IEEE Access
Multidisciplinary | Rapid Review | Open Access Journal

Received September 2, 2020, accepted September 24, 2020, date of publication September 30, 2020,
date of current version October 13, 2020.

Digital Object Identifier 10.1109/ACCESS.2020.3027881

Automatic Coastline Extraction and Changes Analysis Using Remote Sensing and GIS Technology

MUHAMMAD YASIR[1], HUI SHENG[2], HONG FAN[3], SHAH NAZIR[4], ABDOUL JELIL NIANG[5], MD. SALAUDDIN[6], AND SULAIMAN KHAN[4]

[1]School of Geosciences, China University of Petroleum at Qingdao, Qingdao 266580, China
[2]College of Oceanography and Space Informatics, China University of Petroleum at Qingdao, Qingdao 266580, China
[3]State Key Laboratory of Information Engineering in Surveying, Mapping, and Remote Sensing, Wuhan University, Wuhan 430079, China
[4]Department of Computer Science, University of Swabi, Swabi 23430, Pakistan
[5]Department of Geography, College of Social Sciences, Umm Al-Qura University, Makkah 24243, Saudi Arabia
[6]Department of Geography and Environment, Jagannath University, Dhaka 1100, Bangladesh

Corresponding author: Hui Sheng (sheng@upc.edu.cn)

This work was supported in part by the National Key Research and Development Program under Grant 2017YFC145600, and in part by the National Natural Science Foundation of China under Grant 41776182.

ABSTRACT This study highlights the coastline position changes of Qingdao coastal area from 2000 to 2019, using GIS and remote sensing technologies through Digital Shoreline Analysis System and LANDSAT images. Understanding the coastline movement by suitable method is an important challenge for this extremely dynamic coast. The shoreline changes were statistically measured using three techniques, namely; Linear Regression Rate, End Point Rate and Net Shoreline Movement. For the automatic coastline extraction, different methods were applied, but among them most suitable techniques is the canny edge algorithm technique, which gives the accurate result. The result show maximum accretion reached was 266.07m/yr, 2391.85m,124.47m/yr for End point rate, net shoreline movement and linear regression rate, respectively. While, the maximum erosion was -142.55m/yr, -1234.59m, -63.22m/yr for End point rate, net shoreline movement and linear regression rate, respectively. This paper hence presents the monitoring processes of coast and analyzing the coastline change by the use of geospatial techniques that would be helpful for the coastal planning and management of the Qingdao coast. The applicability of the proposed model is tested with other generic edge detection algorithms that include; Sobel, Prewitt, and Robert edge detection techniques and it was concluded that our model outperforming in accurately detecting the coastline.

INDEX TERMS Coastline detection, canny edge detection, digital shoreline analysis system (DSAS), GIS, remote sensing, and change detection.

I. INTRODUCTION

The coastline is the meeting line of sea with land by the side of a definite tidal elevation point, that is one of the most significant landform as well as an essential attribute of earth surface, which might be changed in a very short period of time [1]–[4]. A sum of geological impacts like sediment accumulation of oceans and rivers, interaction and different ocean and weather condition; in addition to anthropogenic impacts [5] forms it. As an intermediate line among land and water, coastline along with coastal region is reflected as one of the very complex, dynamic as well as unsteady geomorphic component in the shore environment, which is prejudiced with marine as well as terrestrial forces and alters the coastal landforms. The shoreline fluctuations depend on several factors such as wave action, sedimentation by longshore currents, geomorphology, geology beside the coastline, variations in oceanic level as well as man-made events [6]–[11]. The shore zone has vast significance in human life as a great number of researches that a larger proportion of biodiversity lives and interacts with the beach determine it [12].

The coastal area generally focuses better economic, social and recreational opportunities [13]. It is of great significance for the economic development and natural environment, in spite of offering higher risk of natural disasters, like tsunamis, dangerous waves and coastal erosion [14]. In recent

The associate editor coordinating the review of this manuscript and approving it for publication was Geng-Ming Jiang.

decades, the coastal area was continuously changing under the roles of man-made activities (like sand excavation) and natural influences (like sea-level rise, storm surge) [15]–[17]. It is a very dynamic geomorphic system where constant modification happens at varied spatial and temporal scales [18]. On a medium-term, the erosion of coastal area started from the 1970's and converted into a very severe problem at 1990's [16], [21]. The dramatic decrease of sediment supplies from rivers due to the dam building caused rapid erosion at the delta and estuary areas, especially in the abandoned Yellow River Delta, coastline retreated up to 250 m/a.

In last 3 decades, in China the coastal erosion has become an obstacle hindering economic growth [19], [20]. It creates loss of beach and scenic quality deterioration. In reaction to such difficulties, the government has made important progress during the last few decades for implementation and integrated management, so as to attain sustainable development in coastal regions [21]–[23].

Remote sensing satellite images have been extensively used to monitor position of shore zones and coastline, which deliver repeated and consistent statistics of coastal variations. GIS is one of the essential tools for any modification detection monitoring studies on temporal scale by delivering the information in digital structure [24]–[32]. Numerous researchers utilizing remote sensing data have confirmed its efficiency in understanding several shore processes in addition to coastline dynamics [33]–[37]. Rise of sea level and its impacts on shore landforms are the continuing process of global warming. Global mean sea level (MSL) is expected to increase by 9 to 88 cm up to 2100 [38]. For example, in Thailand over the last few decades a 2,637 km long coastline have been altered, whereas in 2007, the World Bank measured that the Thailand coastline has been lost 2 km^2 per year with the damage of 6 billion bhat[1] for sea level rise. Furthermore, in the last decade, changing of Thailand coast and Andaman seacoast were 15.8% and 37% respectively [39]. Anthony *et al.* [40] specified that over 70% of the world's coasts suffered from erosion. Due to changing climate, the trend of erosion was projected to increase under the situation of sea level rising [41].

Shandong, surrounded by the Bohai Sea and the Yellow Sea, has 3345 km coastline with wide diversity from rocky, sandy to muddy/silty coast. The municipal-level divisions that have a coastline are, from the north, going clockwise: Dongying, Binzhou, Yantai, Weifang, Qingdao, Rizhao and Weihai. The coastline consists of 1278 km artificial shoreline, 25 km estuarine shoreline and 2053 km natural shoreline. Of the natural shoreline, 43.49% is rocky coast (887 km), 36.98% is sandy coast (754 km), and 19.53% is silt-muddy coast (398 km). Generally, the rocky coasts are distributed mainly in the eastern edge, sandy coasts are mainly distributed at the north and south of peninsula as well as the pocket beaches between the headlands to the east, and silt-muddy coasts are mostly distributed in the northwestern coast from Yellow River Delta to Laizhou Bay. More than 1200 km natural coasts of Shandong are under serious erosion, including the rapid erosion area in the abandoned Yellow River Delta, the pocket beaches at the north of the Shandong Peninsula, and the straight sandy coast at the south of the Peninsula [16], [20]. Coastal erosion started from the 1970's and accelerated after 1980's with the increasing coastal economy development. The dramatic decrease of sediment supplies from rivers due to the dam building triggered speedy erosion at the delta and estuary parts, particularly in the abandoned Yellow River Delta, coastline retreated up to 250 m/a [42], [43].

Maximum of the sandy coasts beside the Peninsula were under erosion, because of lack of sand supply from nearby rivers and along-shore sediment transport, and sand dredging from the beach or the adjacent offshore area instigated severe erosion during short period of time. Rise in Sea-level cause sluggish but persistent shoreline retreats and developed a more severe threat. Various kinds of hard and soft solutions for protection coastal areas against erosion were practiced in Shandong [16], [21].

The current study objectives are;

- To develop a novel based approach for the automatic and accurate extraction of coastline using canny edge detector and use GIS as well as remote sensing to assess temporal and spatial variations in the Qingdao coastline from 2000 to 2019.
- To evaluate fluctuation of the position in coastline by digital shoreline analysis in addition to the erosion-accretion calculations.
- To test the applicability of the proposed algorithm by comparing it with other generic edge detection methods such as; Prewitt, Sobel, and Robert edge detection algorithms based on the performance measures that include, NSM, LRR, and EPR.

A. STUDY AREA

1) LOCATION

Qingdao is situated in the southeast of the Shandong Peninsula, positioned at 119° 30' ∼ 121° 00' east longitude, 35° 35' ∼ 37° 09' north latitude, in the east and south bordering the Yellow Sea, beside Yantai City in the northeast, and bordering in the west to Weifang City, Southwest borders with Rizhao City (Figure 1); an entire area of 11,282Km^2 [44].

2) GEOLOGICAL SETTING

The tectonic position of Qingdao is the secondary structural unit of the Xinhuaxia uplift zone—the northeast margin of the Jiaonan uplift and the central and southern part of the Jiaolai depression. The entire Paleozoic stratum and part of the Mesozoic strata are absent in the area, but the Cretaceous Qingshan Formation volcanic rock layer is well-built and is exposed widely in Qingdao. The Proterozoic Jiaonan rose-sea gneiss granite and the late Mesozoic Yanshan granite diorite and Laoshan granite dominate the magmatic rocks.

[1]Thailand currency

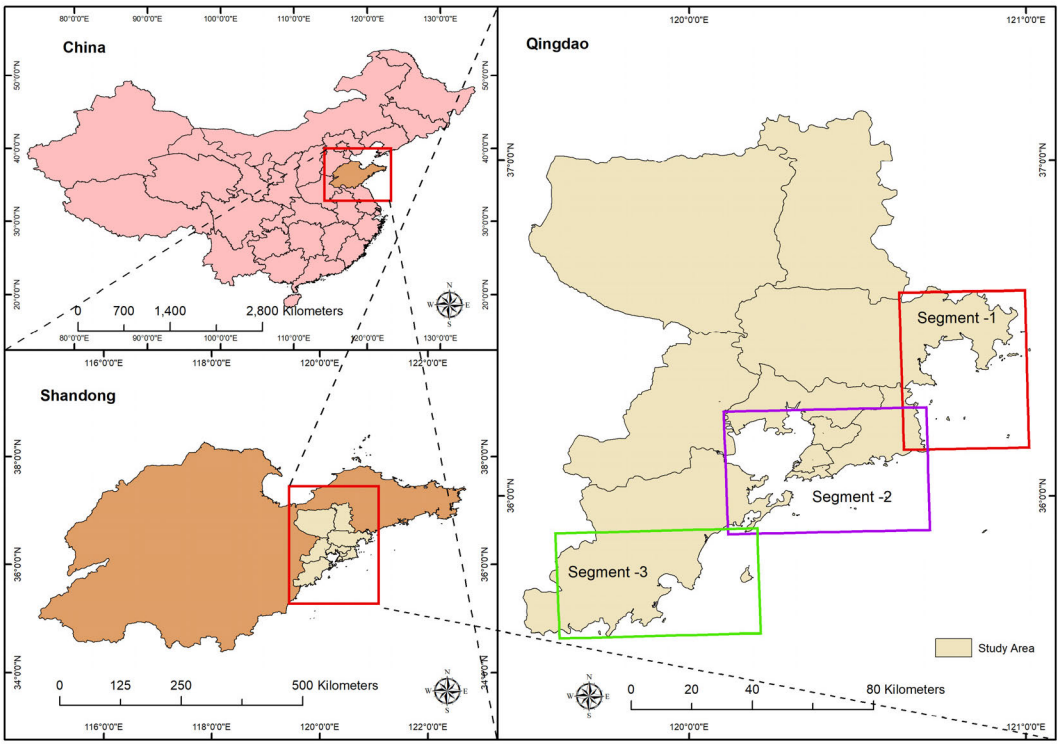

FIGURE 1. Geographic position map of the Study area (Qingdao, East China).

The urban areas are all situated on this type of granite, and the building foundation conditions are excellent. The structure is dominated by faulted structures. Since the Tertiary period, the area is dominated by relatively stable fault block uplifts, and the increase is generally not large [44], [45].

II. RELATED WORK

Currently, there are several studies in the literature on defining coastline changes happening in coastal areas, assessing the future situation of the coastline, and inspecting causes that produce change in coastline. The Digital Shoreline Analysis System (DSAS) is one of the most broadly utilized techniques for the analysis of such studies in the world.

The rates of change of the shoreline were calculated using two approaches integrated to the Digital Shoreline Analysis System (DSAS). The DSAS generate orthogonal transects along the coast and calculate change statistics accordingly, using six distinct approaches including End Point Rate (EPR), Net Shoreline Movement (NSM) and Linear Regression Rates (LRR). A short-term analysis (EPR) was applied using successive shoreline pairs. The EPR statistics result are calculated by dividing the distance of shoreline movement by the time elapsed between two dates. The advantage of this algorithm is that it requires only two shoreline dates for its computation, its inconvenience appears when there are many shorelines, all intermediate shorelines dates are ignored. The only difference between EPR and NSM is that the distance between successive shorelines pairs (the youngest and the oldest) is the total distance and not this distance divided by the time elapsed between the two shorelines. Then they have the same advantages and disadvantages.

A long-term analysis (Linear Regression Rates -LRR) exploits all shorelines and has been used to calculate shoreline changes for 19 years from 2000 to 2019. The LRR rate-of-change statistic can be determined by fitting a least-squares regression line to all shoreline points. The advantages of this method are multiples: all shorelines are used, the method is purely computational and the calculation is based on accepted statistical concepts [58]. The disadvantage of this method does not take into account shifts between intervening periods that may slow down or accelerate trends. Average short-term change rates (EPR) fill this gap and highlight all trends for all transects between the different time periods.

Niang [46] presented the coastline position deviations at Yanbu shore region from 1965 to 2019, utilizing multitemporal satellite imageries and applied DSAS. The variation rates of coastline were measured based on WLR, LRR, NSM as well as EPR, statistical approaches to measure the long and short term trends. The extreme accretion was noted 1655.9 m (30.66, 32.32 and 36.9 m/year based on EPR, LRR and WLR techniques, respectively), whereas the extreme erosion was recorded as −1484.8m (−37.9 m/year, −32.7 m/year and −33.5 m/year based on EPR, LRR and WLR techniques, respectively). An area of around 20 km^2 of sea and islets has been dug or backfilled in for numerous activities.

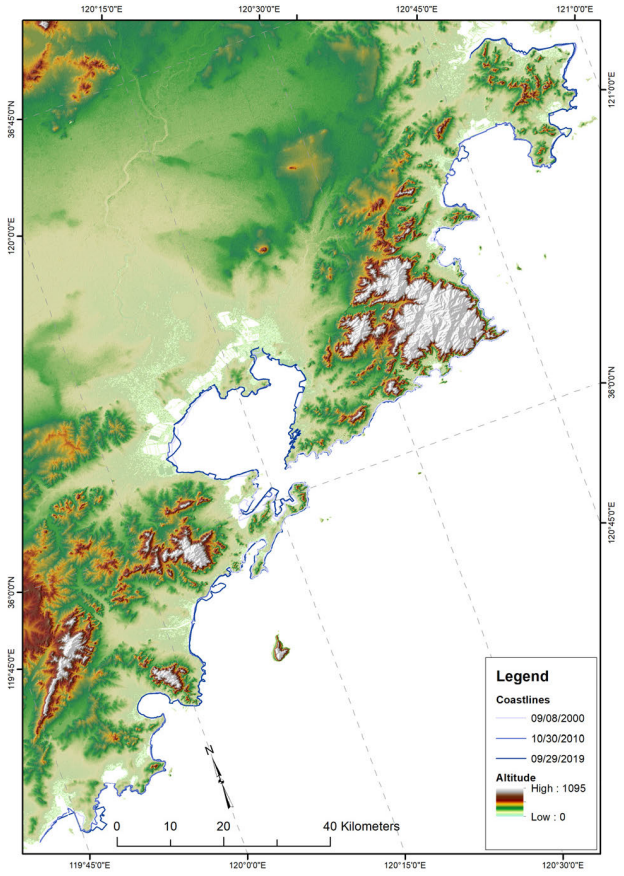

FIGURE 2. Topographic setting of study area, (DEM SRTM).

Nassar *et al.* [47] detected the North Sinai coastline change in Egypt with Landsat satellite imageries by the use of DSAS. Ciritci and Türk [48] assessed the Göksu Delta coastline fluctuations with Landsat satellite imageries and GIS-based analyses. They examined variations in coastal zone that happened from 1984 to 2011 (1984, 1998, 2003, 2006, 2011) with confidence interval of 95% by the help of the LRR, SCE and EPR techniques in the DSAS. Arockiaraj *et al.* [49] revealed the shoreline modification on the Ganapathypule and Bhatye shores of the Ratnagiri area situated on the western coast of India for the year 2014 and 2015 by the use of NSM technique in DSAS. Thang *et al.* [50] determined the coastline variation on the Kien Giang shore in Vietnam by applying the DSAS. Being analyzed, they noticed the quantity of erosion on the Kien Giang shore to be average 4.8 m/year and the quantity of accretion to be about 5.7 m/year in the forty years which covers the time period from 1973 to 2013. Güneroğlu [51] Studied morphological fluctuations that happened in the beach area of Trabzon (Turkey) in four various stages from 1984 and 2011. The investigator used Landsat satellite imageries for the assessment of coastline variations and measured coastline fluctuations that happened over 27 years by the use of DSAS. About 897 transects were created at 100-m pauses in the study area. Every coastal district was analyzed separately, and the related statistics were measured. The investigator had chosen the LRR technique to lessen the consequence of random error and short-term fluctuations.

Ali and Narayana [52] have been evaluated the coastline variation that happened in Trinket Island because of the tsunami tragedy that occurred in India in 2004, by using satellite imageries for the years 2004–2013 and applying the NSM, EPR, and LRR, as well as techniques in the DSAS. From their study, they highlighted that the quantity of erosion was more leading than the accretion quantity, and the average coastline erosion was observed to be −9 m/year. Beyazıt [53] studied shoreline alterations that took place in the Kızılırmak Delta between in the years1987 and 2011. The investigator practiced the band rating method for the coastlines assessment as well as LRR, EPR and the shoreline change envelope (SCE) analysis techniques involved in DSAS for shoreline changes determination. He noticed a movement in the land direction, of which extreme erosion rate was 655.6 m with −27.38 m/year between 2011 and 1987 in the coastline of Kızılırmak Delta. Kuleli *et al.* [54] accomplished the shoreline variation analysis in Turkey's Ramsar wetlands by the use of DSAS and Landsat satellite imageries. Five various wetlands were nominated for the analysis: Göksu Ramsar, Yumurtalık Ramsar, Kızılırmak wetland and Gediz wetland Yeşilırmak wetland. Form the analysis, important coastline fluctuations were detected in some portions of the study area throughout the three periods (1989, 1999, and 2009). For the duration of the period between 1975 and 2009, the 35.57 km^2 wetland in the Gediz Delta turned into the salt marsh or sea.

Alberti *et al.* [55] examined coastline modifications that took place between the years of 2008, 2006, 2003 and 1956 on the seashore of Galicia in Spain by applying the linear WLR, LRR, NSM and EPR, statistical techniques of the DSAS.

Mukhopadhyay *et al.* [56] analyzed the coastline alteration that happened in the Puri area of India because of accretion and erosion by using Landsat imageries for the year 1972, year 2001, and year 2010 and intended to forecast the future coastline. The study was carried out on a 142-km coastline in the Puri area. Based on experimental interpretations, the investigators practiced the EPR technique to examine the coastline and the rate of variation in the coast position in the future. They noticed that the quantity of erosion along Kushabhadra in the north of Puri and on the Chandrabhaga shore was very high and projected short-term and long-term for years 2015 and 2025 coastline positions respectively. Sheik and Chandrasekar [57] explored fluctuations of coastal areas in South India by DSAS application. According to hydrological and geological features, they distributed the whole study area into four different coastal areas and utilized IRS and Landsat satellite data (1999 to 2009 by keeping 2 years of gap between each period) for the coastline extraction. After coastline change analysis, in the study area the erosion was detected to be very dominant.

III. MATERIALS AND METHODS

In this research work, the pre-processing steps are applied for the automatic extraction of coastline by using the ENVI 5.3

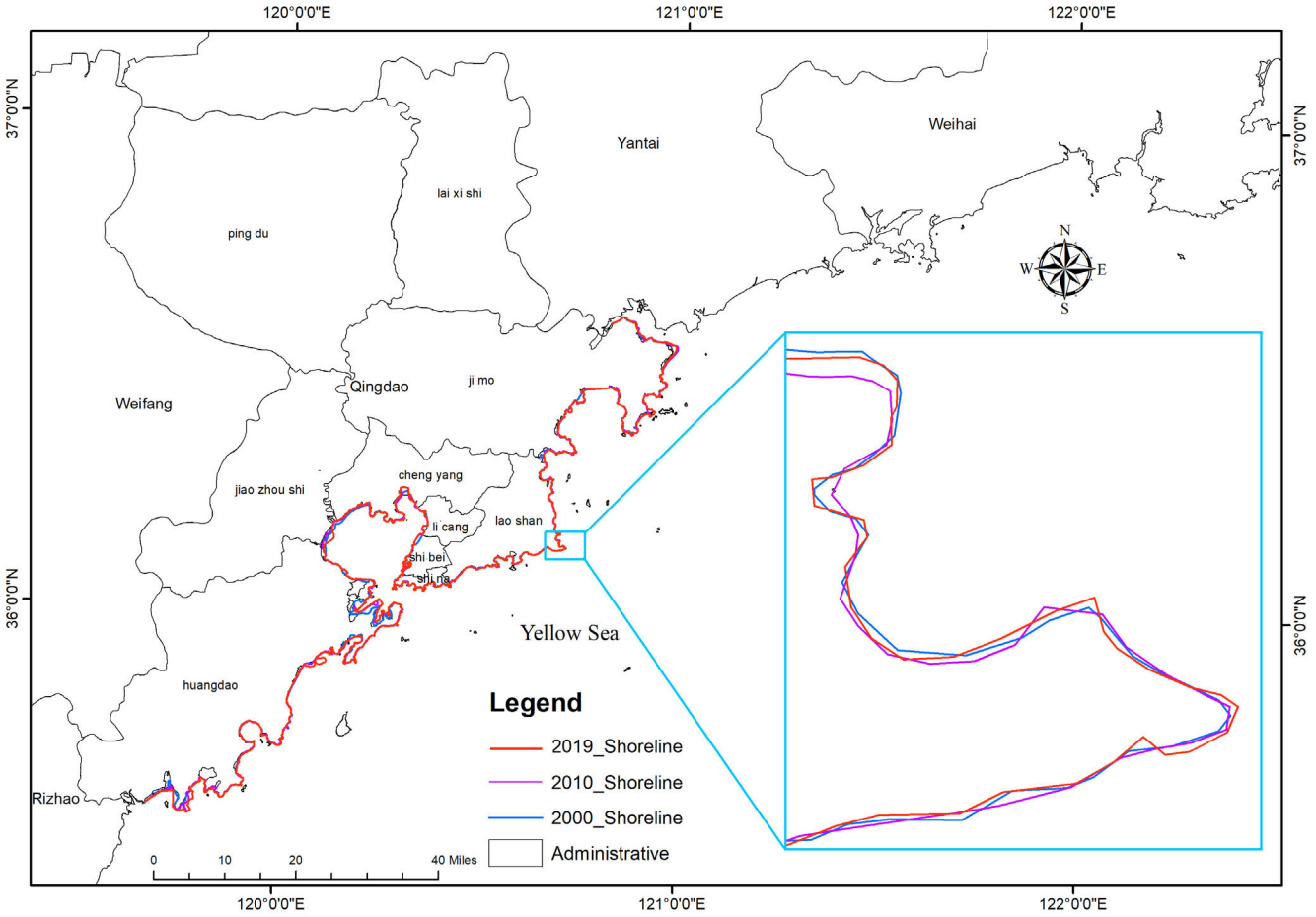

FIGURE 3. Spatial distribution of Qingdao coastline, East china.

software, and MATLAB 2019. The shoreline change analysis was performed using ArcGIS 10.5 and DSAS 5.0. Furthermore, the erase tool of ArcGIS practiced for the calculation of erosion-accretion of the study area.

The steps of process used in the study are visualized in Figure 7.

A. DATA SOURCES

In the proposed research work, Landsat Multi-temporal satellite data (Operational Land Imager - OLI) and Enhanced Thematic Mapper Plus – ETM+ sensors) are used to cover the study area in 2000, 2010 and 2019. The images were freely acquired from the US Geological Survey's (USGS) Earth explorer website (http://earthexplorer.usgs.gov). Because of the open accessibility and affordability of medium spatial resolution, Landsat imageries were selected for current study. Table 1 depicts detail regarding the data. For this study the data is pre-processed by USGS and delivered level-one terrain-corrected (LIT) Landsat data in WGS84 geodetic datum, Universal transverse Mercator Map projection (UTM, Zone 51N), because of the LIT nature of the data the radiometric and geometric deformation were previously rectified before provision [59]–[61].

TABLE 1. Landsat datasets details utilized in this study.

Year/ Month	Sensor	Path/ Row	Spatial Resolution (m)	Cloud	No of Band	Format
08/9/2000	Landsat_7 ETM+	120/35	30	O	7	Geo TIF
29/10/2010	Landsat_7 ETM+	120/35	30	0	7	Geo TIF
29/9/2019	Landsat_8 OLI	120/35	30	0	11	Geo TIF

B. THE AUTOMATIC COASTLINE EXTRACTION

First of all, the pre-processing steps, which comprised of radiometric correction and fast line-of-sight atmospheric analysis of hypercubes (FLAASH) phases, were applied to satellite imageries. Secondly, a digital index i.e., the Normalized Difference Water Index (NDWI) was used to distinguish land features and water.

1) SEGREGATION OF NON-WATER AND WATER ATTRIBUTES BY MEANS OF SPECTRAL INDEX

The multi-temporal LANDSAT imageries were utilized in present study, an appropriate index containing common bands

from all sensors i.e., ETM, OLI were considered. Near infrared and Green band are common bands at Landsat 7 and 8 sensors. Hence, [62] Mcfeeters (1996) NDWI is suggested. NDWI for describing water features has better accuracy compared to other indices as NDWI between manually and theoretical adjusted threshold are most accurate [63]. Eq. (1) was used for measuring NDWI (62).

$$NDWI = \frac{Green_{BOA} - NIR_{BOA}}{Green_{BOA} + NIR_{BOA}} \tag{1}$$

Here, $Green_{BOA}$ and NIR_{BOA} represent reflectance of green and Near Infrared bands, respectively.

The value of NDWI ranges from -1 to $+1$. The image of NDWI usually for water feature provides positive result and for non-water feature negative [62]. Only non-water and water features are mandatory to demarcate the line of separation as a coastline and thus a binary image classification i.e., 0 and 1 was carried out for portraying non-water and water features [64] Figure 4, 5 and 6.

2) CANNY EDGE ALGORITHM

Afterward, in order to achieve the coastline extraction from remote sensing images, there are many methods for image edge detection commonly operators are Sobel, Prewitt, Robert and Canny. These are the implementation of the algorithm is simple and the detection is fast. Among these methods, we use the canny edge algorithm to extract accurate automatic coastline as a substitute of time consuming on-screen digitizing.

Automatic extraction of coastline is very vital as, if the study area is very indented and large, it might take a lengthy time to manually extract the coastline. For instance, the current study area is indented and very huge it has a coastline of about 526 km. Simultaneously, manual extraction of the coastline of 3 periods will cause substantial loss of time.

The canny edge detection method based on the optimization idea can make up for the deficiencies of other gradient operators. It is consider the most successful and the most widely used gray-scale edge detection method. This paper has analyzed the remote sensing image edge detection; the canny method follows the detection steps of the canny method to complete the edge extraction. So, Canny is considered as the best edge detection operator to extract the clearest image edge, with excellent continuity and no break points in principle. Sea and land boundaries in the satellite images are ladder-type edge that is transformed from land to seawater when the gray values of the image will change. This feature was in line with the canny operator edge positioning accuracy. Canny outperforms in achieving accurate coastal line with a limited time and iterations compared to other edge detection algorithms.

The detection step of the method completes the extraction of the edge. The canny method has four main steps in implementation [65].

- Smooth image with noise reduction. Use Gaussian function $G(x, y)$ to convolve image $f(x, y)$ Get smooth image $g(x, y)$, as

$$G(x, y) = \frac{1}{\sqrt{2\pi}\sigma} \exp\left(\frac{-(x^2 + y^2}{2\sigma^2}\right) \tag{2}$$

$$g(x, y) = f(x, y) * G(x, y) \tag{3}$$

  where α is the smooth scale parameter
- Compute the gradient direction and amplitude. Use an appropriate gradient operator to measure the gradient size and direction of every pixel of the image after noise reduction.
- Non-maximum suppression (NMS), so as to accurately locate the position of the edge point, the non-maximum suppression method is adopted for the gradient value of each pixel. In the neighborhood of the current pixel, by comparing the gradient amplitude of the consecutive points, it was concluded that a greater amplitude value represents a corresponding edge at the point of interest and for a small amplitude value; it is arbitrated as no-edge at that point.
- High/low threshold detection and edge connection, through the above steps; the edges obtained after the processing are only rough edges, and the high/low threshold to remove the false edge points must detect them. The points that are less than the low threshold are excluded, and the points that are greater than the high threshold are determined as edge points. Weak points are marked

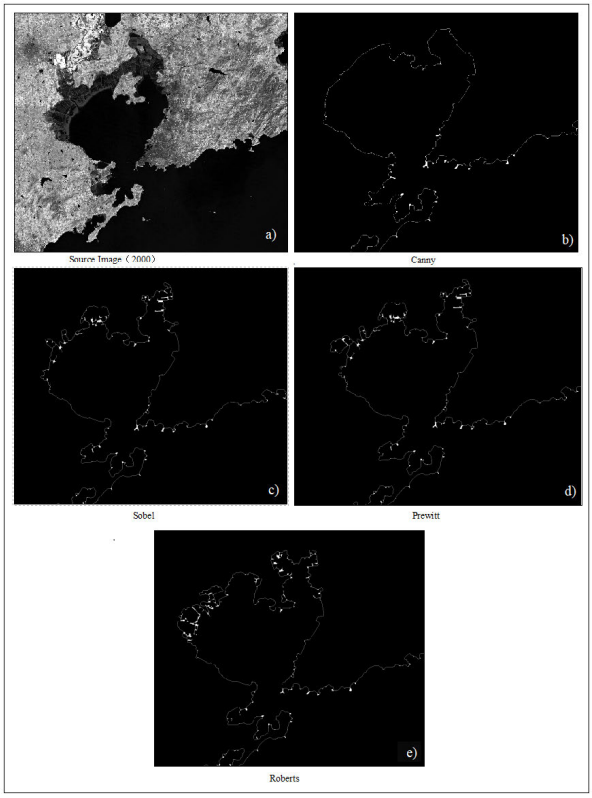

FIGURE 4. Coastline extraction results for 2000 image, a) Greyscale image, b) Canny, c) Sobel, d) Prewitt and e) Robert.

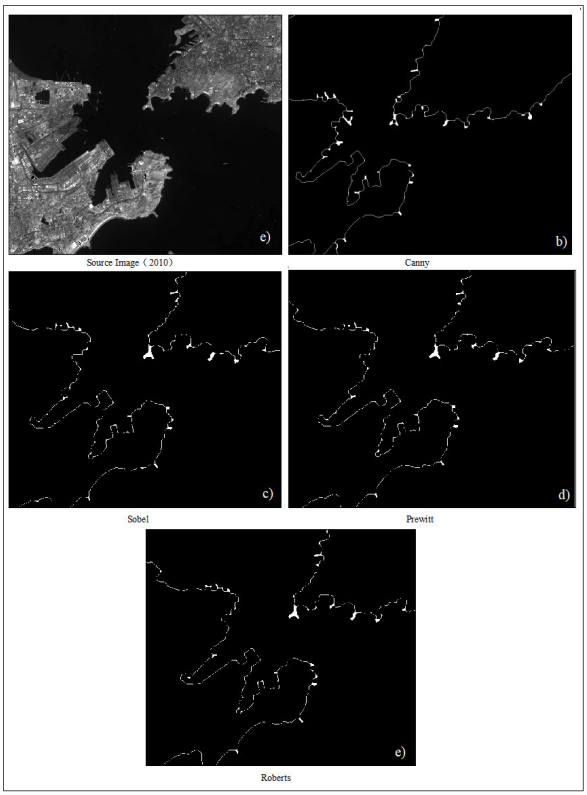

FIGURE 5. Coastline extraction results for 2010 image, a) Greyscale image, b) Canny, c) Sobel, d) Prewitt and e) Robert.

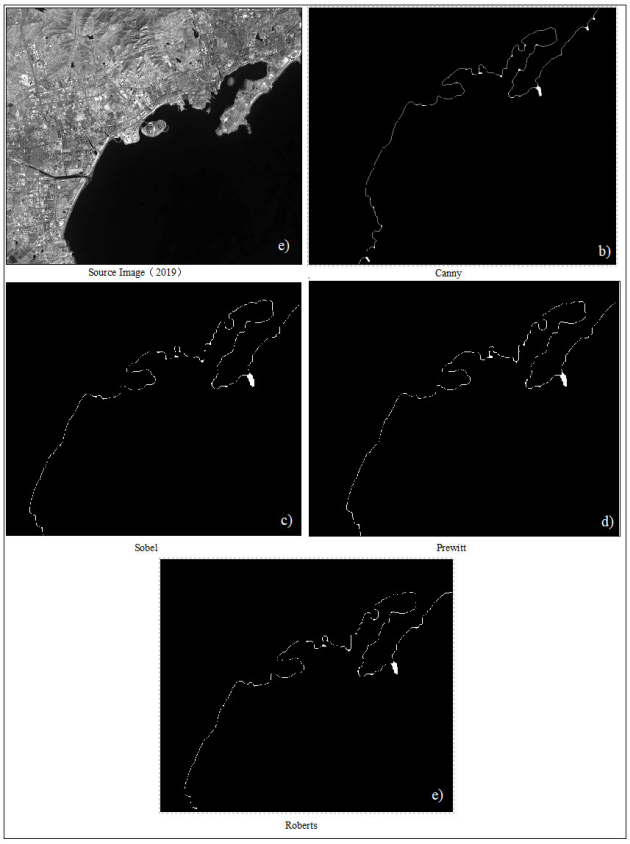

FIGURE 6. Coastline extraction results for 2019 image, a) Greyscale image, b) Canny, c) Sobel, d) Prewitt and e) Robert.

between the two, and then this weak edge is judged whether the point is connected with the edge point. If it is, then this point is recorded as the edge point.

Thus, obtain coastline as vector data and extracted them automatically for each year's (Figure 3).

Figure 4, 5, and 6 represents the edge detection capabilities of each algorithm (Sobel, Robert, Prewitt, and our model) with our model (canny-based model). Based on the finer details in the resultant images and performance metrics of EPR, LRR, and NSM it was concluded that canny-based model (our model) prominent in extracting accurate coastline edges.

C. CALCULATION AND INTERPRETATION OF COASTLINE CHANGE RATES

The Digital Shoreline Analysis System (DSAS) is a GIS-based system established by the USGS. Publicly available, at http://woodshole.er.usgs.gov/project-ages/dsas/. DSAS calculates gaps amongst the coastline positions during defined periods. This offers the basic data to compute the changes of shoreline. The historical trend of these fluctuations of shoreline is based on indicators of the coastline geometry. The system controls the below coastline characteristics: coastline change, historical shoreline dynamics, cliff retreat and erosion, evolution and development of gulls, coastline calculation and modeling [66]. DSAS creates transects that are cast perpendicular to the baseline at a user definite spacing along the coast. The transect coastline intersections along this baseline are then used to compute the rate of change statistics. Based on the logical conditions in DSAS, 5929 transects has been created that are oriented perpendicular to the baseline at each 50m spacing along Qingdao coastline. DSAS 5.0 has six statistical methods to measure variations. In this study, Net shore Movement (NSM), End Point Rate (EPR) and Linear Regression Rate (LRR) approaches were used. NSM measuring net shoreline change according to distance rather than mean value. NSM relates to date and only two shorelines requires, i.e. total distance among the earliest and the latest of coastline in each transect. The End Point Rate (EPR) was selected as the statistical parameter describing the spatial patterns of shoreline change [67]. EPR measures shoreline change by dividing the distance of the coastline among its initial and the most current position of coastline. LRR practices entirely the existing data to calculate long-term rate of variations. Where, the LRR, EPR and NSM positive and negative value shows seaward and landward movement of the coastline respectively. Baseline, historical seashores and coastlines uncertainty are input data delivered in the model for during simulation phase. The spaces among transects alongside the baseline and transects length were demarcated based on the Coastline pattern.

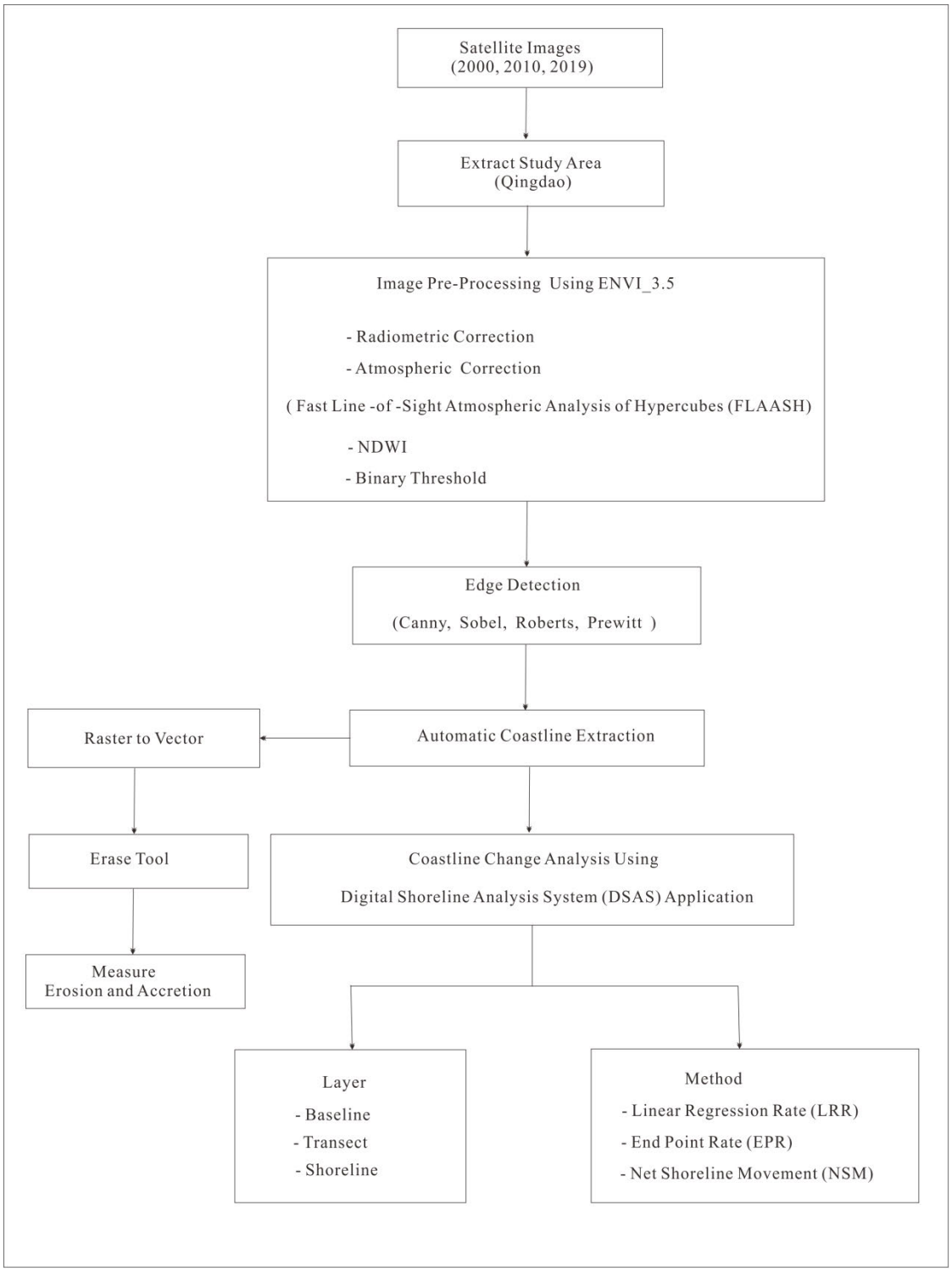

FIGURE 7. Flowchart of the overall methodology adopted to conduct this study.

IV. RESULTS

It is possible to divide the study area into 3 segments, which has a very large and indented. In coastline variation analysis researches, the exploration of the study region by apportioning it into segments offers the chance for an enhanced interpretation of analysis results. For this aim, the study area was inspected by distributing it into three segments figure 1.

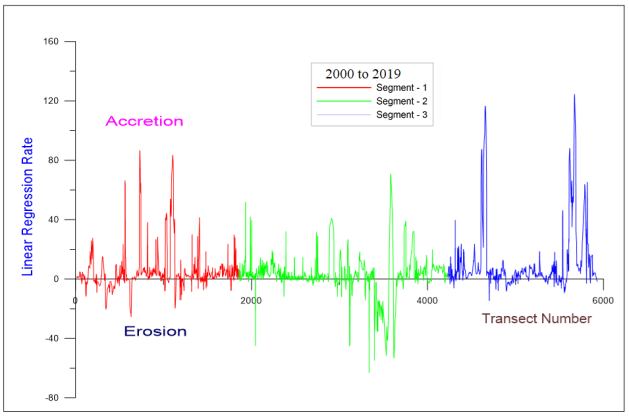

FIGURE 8. Rate of shoreline change (LRR in m/yr) for the year 2000 to 2019.

A. LONG TIME PERIOD ANALYSIS

The coastline change over the period 2000 to 2019 (19 years) was measured using the Linear Regression Rate method (LRR). This tool defines the rate of change statistics by fitting the least square regression to all the shoreline positions from the oldest to newest at every of the transects. The results demonstrated in Figure 8 display the total coastline variation rates measured from the analysis. The coastline progradation shows by positive values whereas the negative values are linked to erosion of coastline. This Figure shows also the position of erosional and accretional parts.

Over the period of 19 years, the LRR total averages rate shows an accretional trend of the coastline for all three segments. The LRR average rates for segment-1, 2 and 3 are 5.1m/yr, 2.9m/yr and 11.54m./yr respectively. Whole averages display that the Qingdao shoreline is largely subject to an accretion. The maximum accretion distance is 124.47m/yr, with a mean rate of 11.54 m/yr. while the erosion maximum distance is -9.2m/yr is found in segment-2 in table 2.

TABLE 2. Segments wise coastline variation from LRR for 19 years using different interval of coastline.

Year	Category	Erosion (m/yr)	Accretion (m/yr)	Maximum (m/yr)	Minimum (m/yr)	Average (m/yr)
2000 to 2019	Segment 1	-4.46	8.72	86.58	-25.52	5.1
	Segment 2	-9.2	7.67	70.84	-63.22	2.9
	Segment 3	-2.5	14.67	124.47	-14.57	11.54

Figure 8 displays the segment-based evolution of the coastline position of the Coastline throughout the study period measured by the LRR technique. Results obtained from this technique are very consistent as evident from the mean value of the rates for all the segments. Analyses also presented that the coastline shifted in the whole study area with variable rates.

B. SHORT TIME PERIOD ANALYSIS

1) COASTLINE CHANGES 2000 TO 2010

The rates of coastline position variations measured by the NSM and EPR methods during this period indicate that the coastline is principally subjected to aggradation.

This general trend varies according to the three segments defined along the coast as exposed in the table 4, 5 and figure 9, which shows a spatial variability in the dynamics of the coastline. The overall averages EPR rates for all segments show an accretional trend with 2.08 m/yr, 0.13 m/y and 2.51m/yr for segment-1, segment-2 and segment-3 respectively. The NSM distance values follow the same trends with 21.09 m, 1.36 m and 25.54 m respectively for segments-1, 2 and 3. The maximum accretion distance NSM values are 821.25m, 979.48m and 1163.15 for the segments-1, 2 and 3 respectively while the maximum accretion EPR rates for the segments in the same order are 80.9 m/yr, 96.6 and 114.7 m/yr. The maximum erosion distance NSM reach -372.46 m, -898.93m and -731.36 m for the segments 1, 2 and 3, respectively and the EPR are-36.73 m/yr, -88.65m/y and -81.86 m/yr for the same segments in the same order.

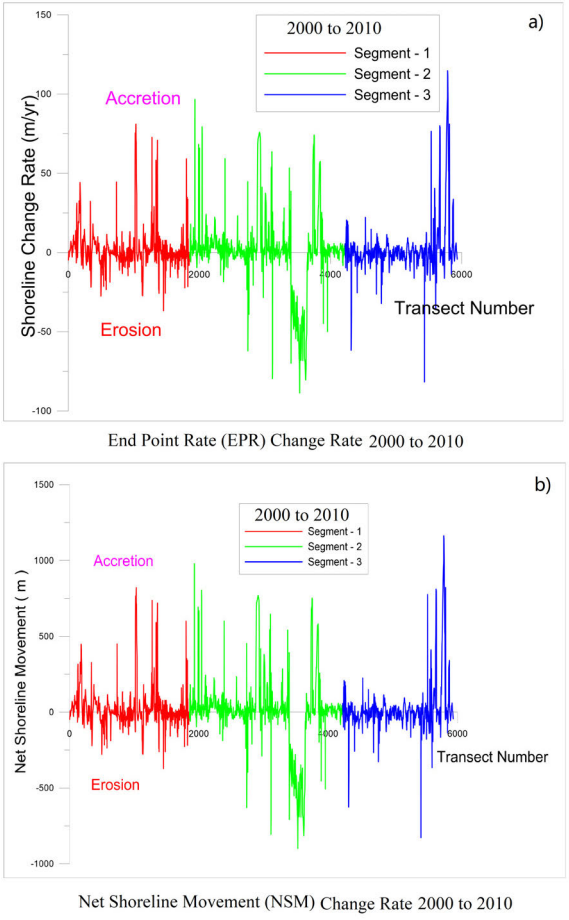

FIGURE 9. a) Rate of shoreline change (EPR in m/yr), b) Net shoreline movement (NSM in m) for the year 2000 to 2010.

This results shows that the segment-2 is less affected by the accretion phenomena, which are more relevant to segment-3.

2) COASTLINE CHANGES 2010 TO 2019

The rates of coastline position changes measured by the NSM and EPR methods during this period specify that the coastline is principally subjected to aggradation:

This general trend varies according to the three segments defined along the coast as exposed in the table 3, 4 and figure 10, which shows a spatial variability in the dynamics of the coastline. The overall averages EPR rates for all segments show an accretional trend with 8.6 m/yr, 6.2 m/y and 21.97m/yr for segment-1, segment-2 and segment-3 respectively. The NSM distance values follow the same trends with 76.73 m, 55.61 m and 195.81m respectively for segments-1, 2 and 3. The maximum accretion distance (NSM) values are 1720.84m, 1869.18m and 2372.01m for the segments-1, 2 and 3 respectively while the maximum accretion EPR rates for the segments in the same order are 193.03m/yr, 209.66 and 266.07 m/yr. The maximum erosion distance (NSM) reach -731.36m, -1270.82m and -121.44 m for the segments-1, 2, 3, respectively, and the EPR are -82.06 m/yr, -142.55 m/y and -26.07 m/yr for the same segments in the same order.

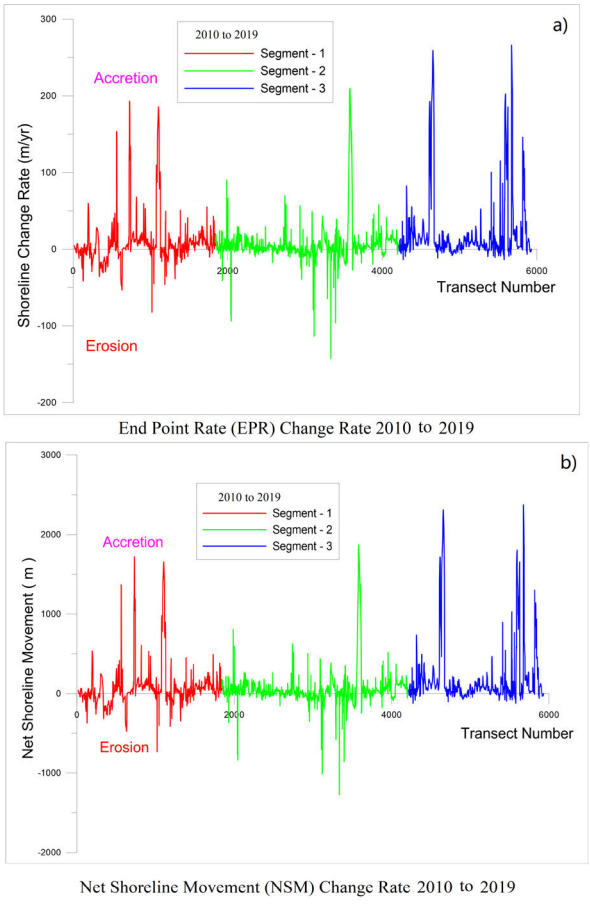

FIGURE 10. a) Rate of shoreline change (EPR in m/yr), b) Net shoreline movement (NSM in m) for the year 2010 to 2019.

TABLE 3. Segments wise coastline variation from EPR for 19 years using various interval of coastline.

Year	Category	Erosion (m/yr)	Accretion (m/yr)	Maximum (m/yr)	Minimum (m/yr)	Average (m/yr)
2000 to 2010	Segment1	-4.65	8.82	80.99	-36.73	2.08
	Segment2	-15.85	9.65	96.6	-88.65	0.13
	Segment3	-4.73	10.2	114.71	-81.86	2.51
2010 to 2019	Segment1	-10.91	18.63	193.03	-82.06	8.6
	Segment2	-6.9	13.48	209.66	-142.55	6.2
	Segment3	-3.2	27.2	266.07	-13.62	21.97
2000 to 2019	Segment1	-4.57	8.82	88.67	-26.07	5.01
	Segment2	-9.2	7.67	73.55	-64.78	2.96
	Segment3	-2.68	14.82	125.53	-14.3	11.64

TABLE 4. Segments wise coastline change from NSM for 19 years using various interval of coastline.

Year	Category	Erosion (m)	Accretion (m)	Maximum (m)	Minimum (m)	Average (m)
2000 to 2010	segment 1	-47.18	89.46	821.25	-372.46	21.09
	segment 2	-160.38	98.04	979.48	-898.93	1.36
	segment 3	-48	103.53	1163.15	-828.3	25.54
2010 to 2019	segment 1	-97.26	166.11	1720.84	-731.36	76.73
	segment 2	-61.42	120.43	1869.18	-1270.82	55.61
	segment 3	-29.08	246.86	2372.01	-121.44	195.81
2000 to 2019	segment 1	-86.18	168.21	1689.57	-496.57	97.44
	segment 2	-176.88	146.15	1401.46	-1234.59	56.12
	segment 3	-49	281.8	2391.85	-272.71	221.72

This results shows that the segment-3 is more affected by the accretion phenomena.

3) COASTLINE CHANGES 2000 TO 2019

The rates of coastline position variations measured by the NSM and EPR methods during this period show that the coastline is principally subjected to aggradation.

In table 3, 4 and Figure 11 the spatial variability in the dynamics of the coastline are shown. The overall averages EPR rates for all segments show an accretional trend with 5.01 m/yr, 2.96 m/y and 11.64 m/yr for segment-1, segment-2 and segment-3 respectively. The NSM distance values follow the same trends with 97.44 m, 56.12 m and 221.72 m respectively for segments 1, 2 and 3. The maximum accretion distance (NSM) values are 1689.57 m, 1401.46m and 2391.85for the segments-1, 2 and 3 respectively while the maximum accretion EPR rates for the segments in the same order are 88.67m/yr, 73.55 and 125.53 m/yr. The maximum erosion distance (NSM) reach -496.57m, -1234.59m and -272.71m for the segments-1, 2 and 3 respectively, and the EPR are -26.07m/yr, -64.78m/y and -14.3m/yr for the same segments in the same order. This results shows that the segment-2 more erosional and less accretion is observed than other segments.

C. LAND LOSS AND LAND GAIN CALCULATION

Qingdao coastline is changing over time because of accretion and erosion process. However, the whole area of the coastline is almost gone through the accretion process whereas the erosion also occurred but not like the accretion through the entire period. From 2000-2019 most of the accretion took place having 52.89 sq. km of the net gain of the area although in this period coastline has lost about 14.40 sq. km of the land. The varying pattern of landmass in diverse interval has presented

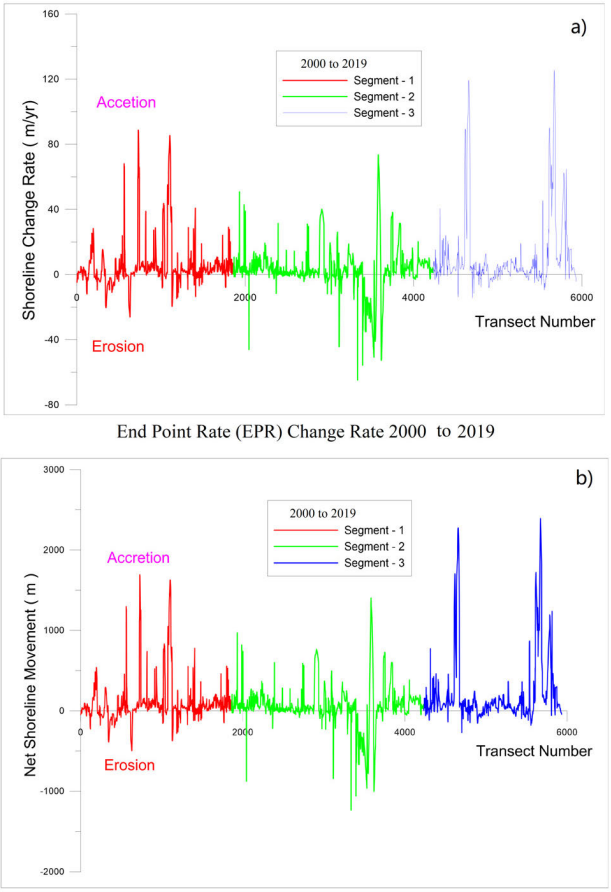

FIGURE 11. a) Rate of shoreline change (EPR in m/yr), b) Net shoreline movement (NSM in m) for the year 2000 to 2019.

TABLE 5. Accretion and erosion (k^{m2}) of Qingdao coastal.

Gain/Loss	2000 to 2010	2010 to 2019	2000 to 2019
Land gain (sq. km)	35.38	42.50	67.29
Land loss (sq. km)	15.88	9.12	14.40
Net Gain/Loss	19.5	33.38	52.89

in Table 5 and Figure 12. In first interval (2000 – 2010), the coastline has increased around 35.38 km^2 of land in 10 years whereas lost only 15.88 km^2 in second interval the coastline has extended about 42.50 km^2 of land in 9 years whereas only lost 9.12 km^2.

V. DISCUSSION

According to the results, in period form, 2000 to 2010 the rates of shoreline position changes indicate that all transects are accretional and less erosion was observed for the entire period as shown in figure 13. Similarly from 2010 to 2019 coastline exposed to the same changes the net accretion rate is denoted higher than the net erosion rate it means that in this period all transects are accretional figure 14, in every segment of this period the shoreline undergone with erosion

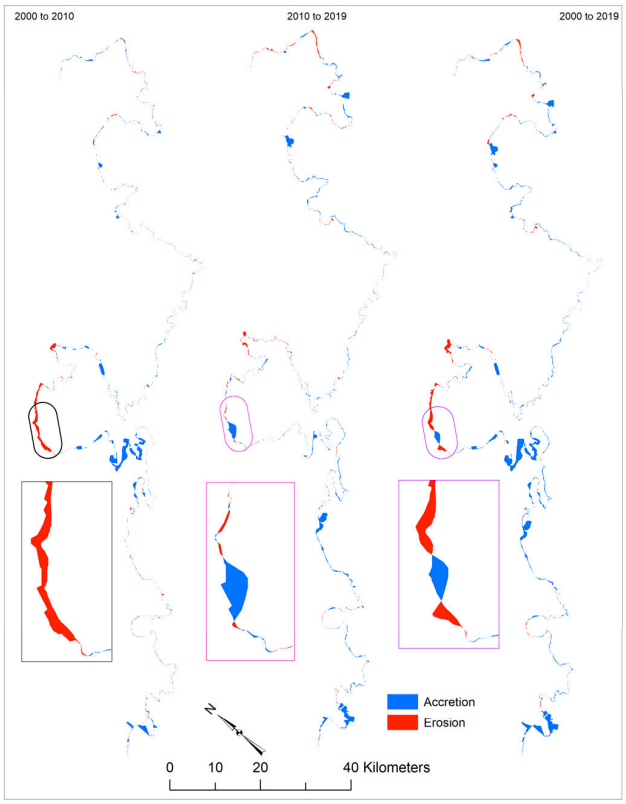

FIGURE 12. Erosion-accretion in study area between the years, a) 2000 to 2010, b) 2010 to 2019, c) 2000 to 2019.

and accretion continuously where the shoreline exposed to the more accretion rate as compared to the erosion. In this, small patches were exposed to more erosion rate while the other parts are less eroded while the accretion was observed at all segments more than erosion.

The overall period from 2000 to 2019 the shoreline of Qingdao faced the erosion and accretion rate here the segment-1 and 3 have observed more accretion than erosion whereas the segment-2 of this period more erosion was detected than accretion as given in Figure 15 in the past two decades the shoreline exposed to various process of erosion and accretion which brought changes in the Qingdao coastline, in this period some part of the coastline observed severe erosion otherwise the accretion rate is dominant throughout the entire period. Figure 16 show major changes of erosion and accretion for diverse periods from 2000 to 2019.

According to the above analysis the main reason for coastline, change in the Qingdao over 19 years was mostly the anthropogenic development, whereas the natural factors were the secondary reasons. The shoreline alteration is produced by a complex interaction of different human-induced and natural coastal practices. The natural processes owing to geomorphology and geology, the combined stroke of currents and waves, storms, tectonics and sea level fluctuation transform the coastlines. The coastal geomorphology and geology

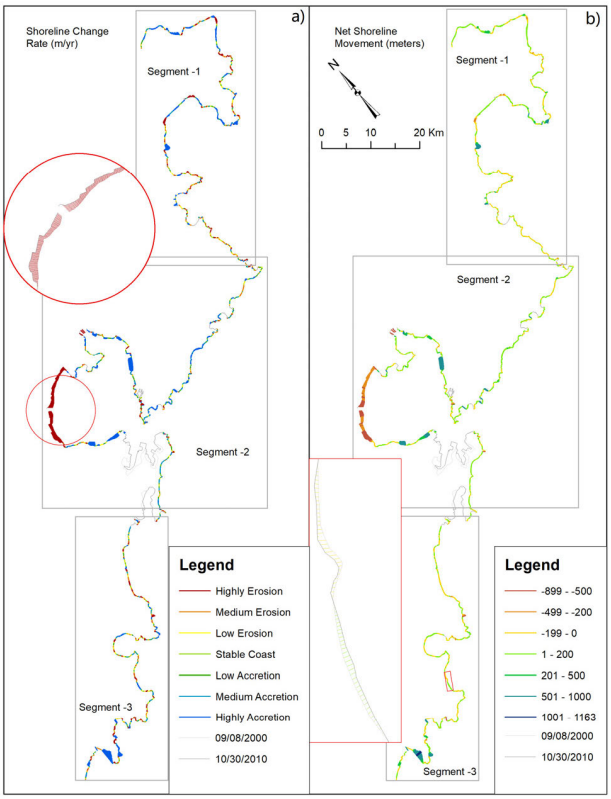

FIGURE 13. a) End point rate (EPR), b) Net shoreline movement (NSM) of Qingdao coastal 2000 to 2010.

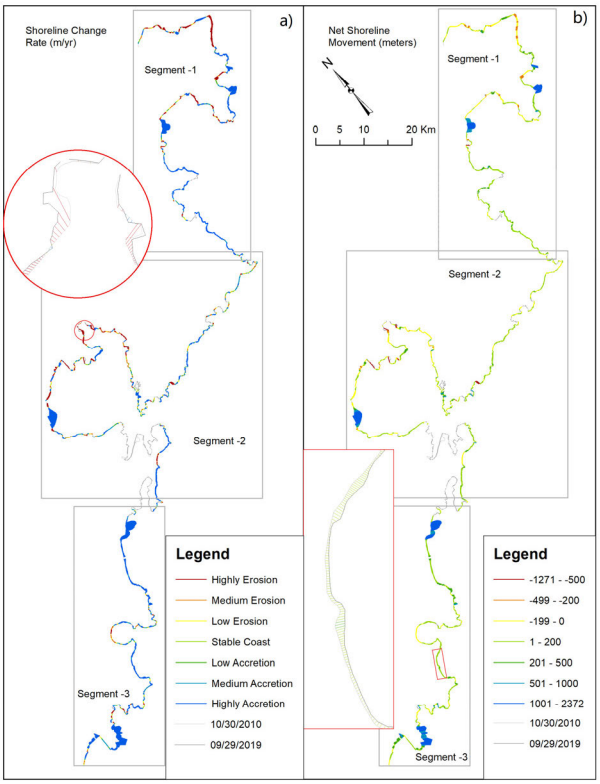

FIGURE 14. a) End point rate (EPR), b) Net shoreline movement (NSM) of Qingdao coastal 2010 to 2019.

plays an energetic role in shorelines modification. The several coastal landforms features, like bays and headland, sand dunes, estuaries, mud flats and beaches and alongside the study area were involved in the coastline fluctuations [68]. The variations in the sea level also can cause erosion or accretion of the shoreline [69]. The current sediment shortage on the coastline owing to natural causes is one of the reasons of erosion [70]. Littoral transport shows main role in the expansion of several coastline landscapes like bars and spits as well as producing substantial coastal accretion and erosion [71]. These days, interventions of human and anthropogenic events also have excessive influence on coastline variations [68]. The key reason of accretion is the deposition of sand on the beach [73]. The only accretion can occur owing to the decreased retreat rate [74] nearby Dai River mouth for the period 1986 to 2000. Accretion with sand deposition was triggered by the tides, wind, movement of the waves and longshore current, wind speed, Wind direction and wave action plays an important role in the deposition of sand [75]. The segment-2 of both periods 2000 to 2010 and 2000 to 2019 observed more erosion and it is due to Human activities on the coast can cause local but quick erosion. These activities included sand mining directly from beaches or near-shore area which caused net sand loss in very short time or topography decrease in the near-shore areas which led to stronger wave energy on the beach and sand wash off. Besides that, Influence of sea level rise on the shore erosion appears more certain after decades of global observation, with more certain trend of global warming [76]. Fan and Li [77] have described that there are two kinds of factors that influence coastal erosion: natural ones, like rises in sea level, storm surges and hydrodynamic condition variations as well as anthropogenic ones, like coastal engineering, fluvial sediment trapping, tourism influences and sand dredging.

The uncertainties were observed in the form of unwanted edges calculation (noise) during the simulation phase. To address this problem we applied thresholding process to remove the unwanted edges (noise) to get accurate coastline results. A threshold value of 40 is selected as an optimal value in our case. Greater values than that results in blurring the image and also removes the desired information from the coastline image.

The different sources of uncertainty that affect the accuracy of the positioning of the shoreline and hence the reliability of measurements of the historical evolution of coastlines can be classified into two categories: errors introduced by data sources and those related to methods of measuring and interpreting the coastline [78], [79]. In current study, the shorelines were extracted automatically from LANDSAT images that have been already orthorectified and georeferenced. Thus, the errors related to digitizing and georeferencing can be limited. The errors linked to image resolution can be reduced by applying resolution merge on the Landsat images.

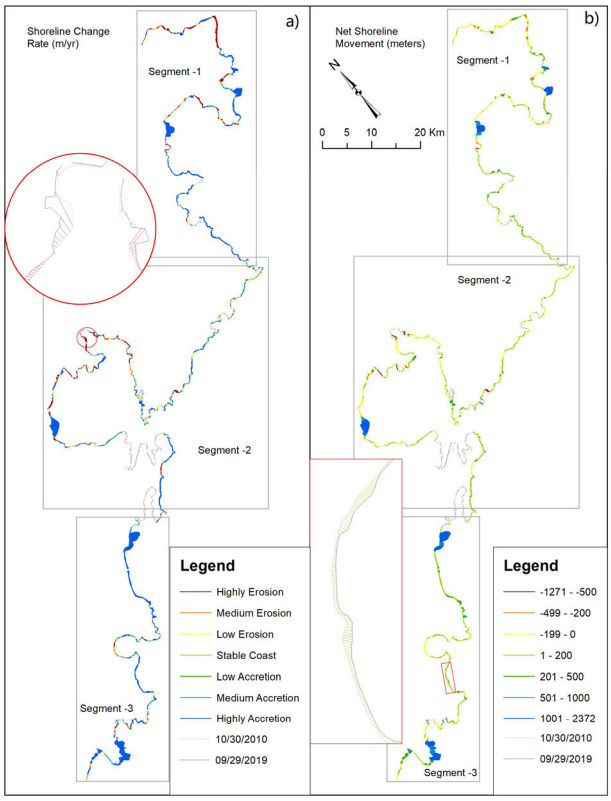

FIGURE 15. a) End point rate (EPR), b) Net shoreline movement (NSM) of Qingdao coastal 2000 to 2019.

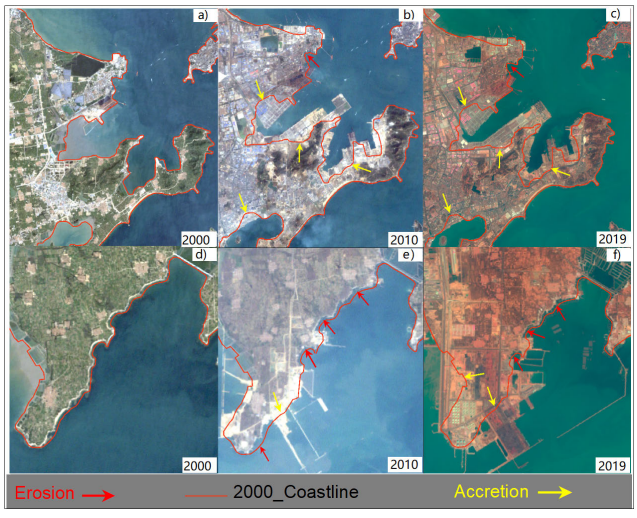

FIGURE 16. Major shoreline change parts along Qingdao coast for diverse periods from 2000 to 2019.

An accuracy graph is generated based on the finer details provided and time consumption by each coastal-line extraction algorithms as depicted in figure 17. It is concluded that Canny outperforms with an accuracy rate of 97.23% that reflects the applicability of the proposed model for the coastal-line extraction and identification.

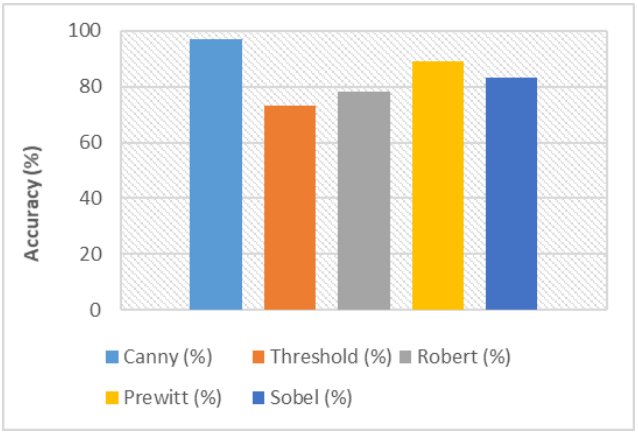

FIGURE 17. Performance analysis of multiple edge detection algorithms.

VI. CONCLUSION

The spatiotemporal assessment of the coastline variation was accomplished in present research work for the Qingdao coastline integrating GIS and RS. Total 19 years (2000 to 2019) data was evaluated Qingdao coastline, using the DSAS application and multitemporal satellite data. For the automatic extraction of the study area, canny-base edge extraction algorithm is proposed in this research work. This algorithm outperforms by providing accurate and finer edges of the coastline. Apparently, accretion is noticeable in the Qingdao coast. For segment definite analysis, the LRR method is an advantageous approach to understand the coastline change; though, EPR method is effective if the coastline observing a constant either seaward or landward movement. The coastline change rates were measured based on EPR, NSM and LRR, statistical techniques to evaluate the long and short-term trends. The extreme accretion noted was 114.71m/yr (for segment-3 of period 2000 to 2019), 266.07 (for segment-3 of period 2000 to 2019) 125.53m/year (for segment-3 of period 2000 to 2019) based on EPR for each period of segment-3, the NSM value for maximum accretion rate was recorded as 1163.15m (for segment-3 of period 2000 to 2019), 2372.01m (for segment-3 of period 2000 to 2019) and 2391.85m (for segment-3 of period 2000 to 2019), while the maximum erosion was for segment-2 -15.85m/year (2000 – 2010), for segment-1 -10.91m/year (2010 to 2019) and for segment-2 -9.2m/yr (2000 – 2019) based on EPR, the NSM value for maximum erosion rate was recorded as -160.38m (for segment-2 of period 2000 to 2010), -97.26m (for segment-1 of period 2010 to 2019) and -176.88 m (for segment-2 of period 2000 to 2019).

The present study identifies the areas of very accretional and eroded area during the period from 2000 to 2019. As a non-structural calculates the spatiotemporal variation of coastline will be a feasible alternate to upkeep planning of the coastal area. Furthermore, the current study will helpful in coastline susceptibility. Over the past 19 years, human actions have had far additional influence on the topography of coastal areas than natural factors, as artificial facilities have

taken over the natural shoreline. Additionally, study where the coastline alteration performs as a main physical influence. It is significant also to keep observing the possible land loss prone parts and take into attention for future tourism and urban planning.

CONFLICT OF INTEREST

The authors proclaim no conflict of interest concerning this paper.

REFERENCES

[1] F. E. Camfield and A. Morang, "Defining and interpreting shoreline change," *Ocean Coastal Manage.*, vol. 32, no. 3, pp. 129–151, Jan. 1996.

[2] A. K. Niya, A. A. Alesheikh, M. Soltanpor, and M. M. Kheirkhahzarkesh, "Shoreline change mapping using remote sensing and GIS," *Int. J. Remote Sens. Appl.*, vol. 3, no. 3, pp. 102–107, 2013. [Online]. Available: http://www.ijrsa.org

[3] M. Schwartz, Ed., *Encyclopedia of Coastal Science*. Springer, 2006.

[4] D. B. Scott, *Coastal Changes, Rapid BT: Encyclopedia of Coastal Science*, M. L. Schwartz, Ed. Dordrecht, The Netherlands: Springer, 2005, pp. 253–255.

[5] E. H. Boak and I. L. Turner, "Shoreline definition and detection: A review," *J. Coastal Res.*, vol. 214, pp. 688–703, Jul. 2005, doi: 10.2112/03-0071.1.

[6] R. W. G. Carter and C. D. Woodroffe, Eds., *Coastal Evolution: Late Quaternary Shoreline Morphodynamics: A Contribution to IGCP Project 274: Coastal Evolution in the Quaternary*. Cambridge, U.K.: Cambridge Univ. Press, 1994.

[7] P. J. Cowell and B. G. Thom, "Morphodynamics of coastal evolution," in *Coastal Evolution: Late Quaternary Shoreline Morphodynamics*. Cambridge, U.K.: Cambridge Univ. Press, 1994, doi: 10.1017/CBO9780511564420.004.

[8] A. M. Fanos, G. M. Naffaa, M. Y. Gewilli, and M. M. Ali, "Long and short term changes of Rosetta promontory, Egypt," in *Proc. Int. Conf. Medit. Coastal Environ. (MEDCOAST)*, Tarragona, Spain, 1995.

[9] A. C. Ibe, "Coastline erosion in Nigeria," Nigerian Inst. Oceanogr. Mar. Res. AC Ibe, Ibadan, Tech. Rep., 1998.

[10] M. Pidwirny, "Fundamental of physical geography, chapter 10: Introduction to the lithosphere: Introduction to Soil," Univ. Brit. Columbia Okanagan, Kelowna, BC, Canada, Tech. Rep., 2006. [Online]. Available: https://www.phyisicalgeography.net/physgeoglos

[11] P. K. Pandian, S. Ramesh, M. V. R. Murthy, S. Ramachandran, and S. Thayumanavan, "Shoreline changes and near shore processes along Ennore coast, east coast of South India," *J. Coast. Res. West Palm Beach*, vol. 20, pp. 828–845, Jul. 2004, doi: 10.2112/1551-5036(2004)20[828:SCANSP]2.0.CO;2.

[12] A. M. Shibly and S. Takewaka, "Morphological changes along Bangladesh coast derived from satellite images," *Proc. Coastal Eng.*, vol. 3, pp. 41–45, Nov. 2012.

[13] N. G. Rangel-Buitrago, G. Anfuso, and A. T. Williams, "Coastal erosion along the Caribbean coast of Colombia: Magnitudes, causes and management," *Ocean Coastal Manage.*, vol. 114, pp. 129–144, Sep. 2015.

[14] J. P. M. Mulder, S. Hommes, and E. M. Horstman, "Implementation of coastal erosion management in The Netherlands," *Ocean Coastal Manage.*, vol. 54, no. 12, pp. 888–897, Dec. 2011.

[15] F. Cai, X. Su, J. Liu, B. Li, and G. Lei, "Coastal erosion in China under the condition of global climate change and measures for its prevention," *Prog. Natural Sci.*, vol. 19, no. 4, pp. 415–426, Apr. 2009, doi: 10.1016/j.pnsc.2008.05.034.

[16] X. Q. Wu, M. Gao, D. Wang, Y. Wang, Q. S. Lu, and Z. D. Zhang, "Framework and practice of integrated coastal zone management in Shandong province, China," *Ocean Coastal Manage.*, vol. 69, pp. 58–67, Dec. 2012.

[17] J. Hinkel, R. J. Nicholls, R. S. J. Tol, Z. B. Wang, J. M. Hamilton, G. Boot, A. T. Vafeidis, L. McFadden, A. Ganopolski, and R. J. T. Klein, "A global analysis of erosion of sandy beaches and sea-level rise: An application of DIVA," *Global Planet. Change*, vol. 111, pp. 150–158, Dec. 2013, doi: 10.1016/j.gloplacha.2013.09.002.

[18] Z. X. Chu, X. G. Sun, S. K. Zhai, and K. H. Xu, "Changing pattern of accretion/erosion of the modern Yellow River (Huanghe) subaerial delta, China: Based on remote sensing images," *Mar. Geol.*, vol. 227, nos. 1–2, pp. 13–30, Mar. 2006.

[19] X. Chen and Y. Zong, "Coastal erosion along the Changjiang deltaic shoreline, China: History and prospective," *Estuarine, Coastal Shelf Sci.*, vol. 46, no. 5, pp. 733–742, May 1998, doi: 10.1006/ecss.1997.0327.

[20] X. H. Wang, Y.-K. Cho, X. Guo, C.-R. Wu, and J. Zhou, "The status of coastal oceanography in heavily impacted Yellow and East China Sea: Past trends, progress, and possible futures," *Estuarine, Coastal Shelf Sci.*, vol. 163, pp. 235–243, Sep. 2015, doi: 10.1016/j.ecss.2015.05.039.

[21] S. Luo, F. Cai, H. Liu, G. Lei, H. Qi, and X. Su, "Adaptive measures adopted for risk reduction of coastal erosion in the people's Republic of China," *Ocean Coastal Manage.*, vol. 103, pp. 134–145, Jan. 2015.

[22] S. Luo, Y. Liu, R. Jin, J. Zhang, and W. Wei, "A guide to coastal management: Benefits and lessons learned of beach nourishment practices in China over the past two decades," *Ocean Coastal Manage.*, vol. 134, pp. 207–215, Dec. 2016.

[23] S. Luo, H. Wang, and F. Cai, "An integrated risk assessment of coastal erosion based on fuzzy set theory along Fujian coast, Southeast China," *Ocean Coastal Manage.*, vol. 84, pp. 68–76, Nov. 2013.

[24] E. T. Balopoulos, M. B. Collins, and A. E. James, "Satellite images and their use in the numerical modelling of coastal processes," *Int. J. Remote Sens.*, vol. 7, no. 7, pp. 905–919, Jul. 1986.

[25] P. J. Mumby, E. P. Green, A. J. Edwards, and C. D. Clark, "The cost-effectiveness of remote sensing for tropical coastal resources assessment and management," *J. Environ. Manage.*, vol. 55, no. 3, pp. 157–166, Mar. 1999, doi: 10.1006/jema.1998.0255.

[26] S. Nayak, "Use of satellite data in coastal mapping," *Indian Cartogr.*, 2002.

[27] J.-H. Ryu, J.-S. Won, and K.-D. Min, "Waterline extraction from Landsat TM data in a tidal flat: A case study in Gomso Bay, Korea," *Remote Sens. Environ.*, vol. 83, pp. 442–456, Dec. 2002, doi: 10.1016/S0034-4257(02)00059-7.

[28] D. K. Stauble, "The use of shoreline change mapping in coastal engineering project assessment," *J. Coastal Res.*, vol. 38, pp. 178–206, Oct. 2003.

[29] H. Yamano, H. Shimazaki, T. Matsunaga, A. Ishoda, C. McClennen, H. Yokoki, K. Fujita, Y. Osawa, and H. Kayanne, "Evaluation of various satellite sensors for waterline extraction in a coral reef environment: Majuro Atoll, Marshall Islands," *Geomorphology*, vol. 82, nos. 3–4, pp. 398–411, Dec. 2006, doi: 10.1016/j.geomorph.2006.06.003.

[30] E. R. Thieler, E. A. Himmelstoss, J. L. Zichichi, and A. Ergul, *Digital Shoreline Analysis System (DSAS) Version 4.0—An ArcGIS Extension for Calculating Shoreline Change* (Open-File Report). Reston, VA, USA: U.S. Geological Survey, 2008.

[31] M. Salauddin, K. T. Hossain, I. A. Tanim, M. A. Kabir, and M. H. Saddam, "Modeling spatio-temporal shoreline shifting of a coastal island in Bangladesh using geospatial techniques and DSAS extension," *Ann. Valahia Univ. Targoviste, Geograph. Ser.*, vol. 18, no. 1, pp. 1–13, Apr. 2018, doi: 10.2478/avutgs-2018-0001.

[32] P. Zuzek, R. Nairn, and S. Thieme, "Spatial and temporal consideration for calculating shoreline change rates in the great lakes basin," *J. Coastal Res.*, vol. 38, pp. 125–146, Oct. 2003.

[33] T. W. Wagner, J. L. Michalek, and R. Laurin, "Remote sensing application in the coastal zone: A case from the Dominician Repulic," Univ. Center, Michigan, Consort. Int. Earth Sci. Inf. Netw. Rep., 1991.

[34] W. Ahmad and D. T. Neil, "An evaluation of landsat thematic mapper (TM) digital data for discriminating coral reef zonation: Heron reef (GBR)," *Int. J. Remote Sens.*, vol. 15, no. 13, pp. 2583–2597, Sep. 1994, doi: 10.1080/01431169408954268.

[35] K. Anbarasu, R. Baskaran, and G. V. Rajamanickam, "Influence of sea level changes in the development of landforms around Chidambaram, Tamilnadu," *Indian J. Geomorphol.*, vol. 4, no. 1, pp. 13–18, 1999.

[36] R. M. Murali and D. Shrivastava, "Monitoring shoreline environment of Paradip, east coast of India using remote sensing," Current 0-5, Tech. Rep., 2009, vol. 97, no. 1, pp. 79–84.

[37] M. Boutiba and S. Bouakline, "Monitoring shoreline changes using digital aerial photographs, quick-bird image and DGPS topographic survey: Case of the east coast of Algiers, Algeria," *Eur. J. Sci. Res.*, vol. 48, no. 3, pp. 361–369, 2011.

[38] *Impacts, Adaptation and Vulnerability in Contribution of Working Group II to the Third Assessment Report of the Intergovernmental Panel on Climate Change*, IPCC, Cambridge Univ. Press, Cambridge, U.K., 2001.

[39] A. Siripong, "Detect the coastline changes in thailand by remote sensing," *Int. Arch. Photogramm., Remote Sens. Spatial Inf. Sci.*, vol. 38, no. 8, pp. 992–996, 2010.

[40] E. J. Anthony, S. Vanhee, and M.-H. Ruz, "Short-term beach–dune sand budgets on the north sea coast of France: Sand supply from shoreface to dunes, and the role of wind and fetch," *Geomorphology*, vol. 81, nos. 3–4, pp. 316–329, Nov. 2006, doi: 10.1016/j.geomorph.2006.04.022.
[41] R. Al-Tahir and A. Ali, "Assessing land cover changes in the coastal zone using aerial photography," *Surv. Land Inf. Sci.*, vol. 64, no. 2, pp. 107–112, 2004.
[42] Z. Chu, "The dramatic changes and anthropogenic causes of erosion and deposition in the lower Yellow (Huanghe) River since 1952," *Geomorphology*, vol. 216, pp. 171–179, Jul. 2014, doi: 10.1016/j.geomorph.2014.04.009.
[43] T. Wu, X. Hou, and X. Xu, "Spatio-temporal characteristics of the mainland coastline utilization degree over the last 70 years in China," *Ocean Coastal Manage.*, vol. 98, pp. 150–157, Jul. 2014.
[44] Accessed: May 14, 2020. [Online]. Available: http://qdsq.qingdao.gov.cn/n15752132/n15752711/160812110726762883.html
[45] Accessed: May 14, 2020. [Online]. Available: http://www.qingdao.gov.cn/n172/n25664338/n26675614/131021110012675027.html
[46] A. J. Niang, "Monitoring long-term shoreline changes along Yanbu, Kingdom of Saudi Arabia using remote sensing and GIS techniques," *J. Taibah Univ. Sci.*, vol. 14, no. 1, pp. 762–776, Jan. 2020.
[47] K. Nassar, W. E. Mahmod, H. Fath, A. Masria, K. Nadaoka, and A. Negm, "Shoreline change detection using DSAS technique: Case of north sinai coast, Egypt," *Mar. Georesources Geotechnol.*, vol. 37, no. 1, pp. 81–95, Jan. 2019, doi: 10.1080/1064119X.2018.1448912.
[48] D. Ciritci and T. Türk, "Automatic detection of shoreline change by geographical information system (GIS) and remote sensing in the Göksu delta, turkey," *J. Indian Soc. Remote Sens.*, vol. 47, no. 2, pp. 233–243, Feb. 2019, doi: 10.1007/s12524-019-00947-1.
[49] S. Arockiaraj, R. S. Kankara, G. U. Dora, and S. Sathish, "Estimation of seasonal morpho-sedimentary changes at headland bound and exposed beaches along South Maharashtra, West Coast of India," *Environ. Earth Sci.*, vol. 77, no. 17, Sep. 2018, doi: 10.1007/s12665-018-7790-y.
[50] N. T. X. Thang, T. V. Thu, and C. D. Woodroffe, "Coastal erosion vulnerability of Kien Giang—The Western Mekong River delta coast in Vietnam," in *Proc. Int. Conf. Globalisation, Climate Change Sustain. Develop.* Hà Tĩnh, Vietnam: Hà Tĩnh Univ., Apr. 2017, pp. 1–9.
[51] A. Güneroğlu, "Coastal changes and land use alteration on northeastern part of turkey," *Ocean Coastal Manage.*, vol. 118, pp. 225–233, Dec. 2015, doi: 10.1016/j.ocecoaman.2015.06.019.
[52] P. Y. Ali and A. C. Narayana, "Short-term morphological and shoreline changes at Trinkat Island, Andaman and Nicobar, India, after the 2004 Tsunami," *Mar. Geodesy*, vol. 38, no. 1, pp. 26–39, Jan. 2015, doi: 10.1080/01490419.2014.908795.
[53] I. Beyazıt, *Kızılırmak Deltasının Zamansal Kıyı Deıişiminin Coğrafi Bilgi Sistemleri Ve Uzaktan Algılama Yöntemleri ile Belirlenmesi*. Yıldız, Turkey: Yıldız Teknik Üniversitesi Fen Bilimleri Enstitüsü, Yüksek Lisans Tezi, 2014.
[54] T. Kuleli, A. Guneroglu, F. Karsli, and M. Dihkan, "Automatic detection of shoreline change on coastal ramsar wetlands of Turkey," *Ocean Eng.*, vol. 38, no. 10, pp. 1141–1149, Jul. 2011, doi: 10.1016/j.oceaneng.2011.05.006.
[55] A. P. Alberti, A. Pires, and L. H. F. Chaminé, "Shoreline change mapping along the coast of Galicia, Spain," *Proc. Inst. Civil Eng.-Maritime Eng.*, vol. 166, no. 3, pp. 125–144, 2013, doi: 10.1680/maen.2012.23.
[56] A. Mukhopadhyay, S. Mukherjee, S. Mukherjee, S. Ghosh, S. Hazra, and D. Mitra, "Automatic shoreline detection and future prediction: A case study on Puri coast, bay of Bengal, India," *Eur. J. Remote Sens.*, vol. 45, no. 1, pp. 201–213, Jan. 2012, doi: 10.5721/EuJRS20124519.
[57] M. Sheik and Chandrasekar, "A shoreline change analysis along the coast between Kanyakumari and Tuticorin, India, using digital shoreline analysis system," *Geo-Spatial Inf. Sci.*, vol. 14, no. 4, pp. 282–293, Jan. 2011, doi: 10.1007/s11806-011-0551-7.
[58] E. A. Himmelstoss, A. S. Farris, R. E. Henderson, M. G. Kratzmann, A. Ergul, O. Zhang, J. L. Zichichi, E. R. Thieler. (2018). *Digital Shoreline Analysis System (Version 5.0): U.S. Geological Survey Software*. [Online]. Available: https://code.usgs.gov/cch/dsas/
[59] J. R. Jensen, *Introductory Digital Image Processing: A Remote Sensing Perspective*, 2nd ed. Upper Saddle River, NJ, USA: Prentice-Hall, 1996.
[60] K. M. Nahiduzzaman, A. S. Aldosary, and M. T. Rahman, "Flood induced vulnerability in strategic plan making process of riyadh city," *Habitat Int.*, vol. 49, pp. 375–385, Oct. 2015.
[61] T. S. Seilheimer, A. Wei, P. Chow-Fraser, and N. Eyles, "Impact of urbanization on the water quality, fish habitat, and fish community of a lake Ontario marsh, Frenchman's bay," *Urban Ecosyst.*, vol. 10, no. 3, pp. 299–319, Aug. 2007.
[62] S. K. Mcfeeters, "The use of the normalized difference water index (NDWI) in the delineation of open water features," *Int. J. Remote Sens.*, vol. 17, no. 7, pp. 1425–1432, May 1996, doi: 10.1080/01431169608948714.
[63] R. T. Das and S. Pal, "Exploring geospatial changes of wetland in different hydrological paradigms using water presence frequency approach in barind tract of west bengal," *Spatial Inf. Res.*, vol. 25, no. 3, pp. 467–479, Jun. 2017, doi: 10.1007/s41324-017-0114-6.
[64] L. Ji, L. Zhang, and B. Wylie, "Analysis of dynamic thresholds for the normalized difference water index," *Photogramm. Eng. Remote Sens.*, vol. 75, no. 11, pp. 1307–1317, Nov. 2009.
[65] J. Canny, "A computational approach to edge detection," *IEEE Trans. Pattern Anal. Mach. Intell.*, vol. PAMI-8, no. 6, pp. 679–698, Nov. 1986.
[66] D. T. Oyedotun, "Shoreline geometry: DSAS as a tool for historical trend analysis," *Geomorphol. Techn.*, vol. 3, no. 2.2, pp. 1–12, 2014.
[67] E. R. Thieler, E. A. Himmelstoss, J. L. Zichichi, and A. Ergul, "The digital shoreline analysis system (DSAS) version 4.0 an ArcGIS extension for calculating shoreline change," U.S. Geol. Surv., Reston, VA, USA, Tech. Rep., 2009.
[68] M. Sheik and Chandrasekar, "A shoreline change analysis along the coast between Kanyakumari and Tuticorin, India, using digital shoreline analysis system," *Geo-Spatial Inf. Sci.*, vol. 14, no. 4, pp. 282–293, Jan. 2011.
[69] R. G. Dean and R. A. Dalrymple, *Coastal Processes With Engineering Applications*. Cambridge, U.K.: Cambridge Univ. Press, 2004.
[70] R. A. Morton, "Accurate shoreline mapping: Past, present, and future: American society of civil engineers," *Coastal Sediments*, vol. 1, pp. 997–1010, Jun. 1991.
[71] E. Sanjaume and J. E. Pardo-Pascual, "Erosion by human impact on the Valencian coastline (E of Spain)," *J. Coastal Res.*, pp. 76–82, Jan. 2005. [Online]. Available: https://www.jstor.org/stable/25737408?seq=1
[72] D. B. King, *The Dynamics of Inlets and Bays*. 1974.
[73] R. Kannan, A. Kanungo, M. V. Murty, and K. V. Ramana, "Shoreline evolution along uppada coast in Andhra Pradesh using multi temporal satellite images and model based approach," *Indian J. Geosynthetics Ground Improvement*, vol. 8, no. 1, pp. 14–19, 2019.
[74] Z. Xue, A. Feng, P. Yin, and D. Xia, "Coastal erosion induced by human activities: A northwest Bohai sea case study," *J. Coastal Res.*, vol. 253, pp. 723–733, May 2009.
[75] G. Sreenivasulu, N. Jayaraju, B. C. S. R. Reddy, T. L. Prasad, B. Lakshmanna, and K. Nagalakshmi, "Coastal morphodynamics of tupilipalem coast, Andhra Pradesh, Southeast Coast of india," *Current Sci.*, vol. 112, no. 04, p. 823, Feb. 2017.
[76] G. Yin, G. Mariethoz, Y. Sun, and M. F. McCabe, "A comparison of gap-filling approaches for Landsat-7 satellite data," *Int. J. Remote Sens.*, vol. 38, no. 23, pp. 6653–6679, Dec. 2017.
[77] D. Fan and C. Li, "Complexities of China's coast in response to climate change," *Adv. Climate Change Res.*, vol. 2, no. 1, pp. 54–58, 2006.
[78] L. J. Moore, "Shoreline mapping techniques," *J. Coastal Res.*, vol. 16, no. 1, pp. 111–124, 2000.
[79] P. Wernette, A. Shortridge, D. P. Lusch, and A. F. Arbogast, "Accounting for positional uncertainty in historical shoreline change analysis without ground reference information," *Int. J. Remote Sens.*, vol. 38, no. 13, pp. 3906–3922, Jul. 2017.